Turkish Journal of Electrical Engineering & Computer Sciences

http://journals.tubitak.gov.tr/elektrik/

Research Article

Turk J Elec Eng & Comp Sci
(2019) 27: 4640 – 4658
© TÜBİTAK
doi:10.3906/elk-1805-108

Global maximum operating point tracking for PV system using fast convergence firefly algorithm

Madhusmita MOHANTY[1], **Sankar SELVAKUMAR**[1]
Chandrasekaran KOODALSAMY[1,*], **Sishajpulikottil SIMON**[2]
[1]Department of Electrical and Electronics Engineering, National Institute of Technology Puducherry, Karaikal, India
[2]Department of Electrical and Electronics Engineering, National Institute of Technology, Tiruchirappalli, Tamil Nadu, India

Received: 16.05.2018 • **Accepted/Published Online:** 01.08.2019 • **Final Version:** 26.11.2019

Abstract: Global maximum operating point (GMOP) tracking is an important requirement of solar photovoltaic (PV) systems under partial shading conditions (PSCs). Though the perturb and observe algorithm is simple and effective, it fails to recognize the GMOP. This paper explores the application of the firefly algorithm (FA) to the maximum power point tracking (MPPT) problem of PV systems. In order to determine the shortest path to reach the GMOP under various PSCs, a new fast convergence firefly algorithm (FA) is proposed. Additionally, the change in firefly position is limited to a maximum value identified based on the characteristics of the PSC. The fast convergence method is guaranteed to find the GMOP, avoiding the local operating point obstacle through a repeated space search technique. Using MATLAB, the algorithm is implemented on a model PV system. An experimental 300-W PV system is developed to validate the operating point of the PV system under various PSCs. The proposed method is tested on a 5-kW solar power plant. The results demonstrate that the proposed MPPT algorithm outperforms particle swarm optimization, FA-based MPPTs, and other methods available in the literature.

Key words: Global maximum operating point, PV panel, fast convergence firefly algorithm, partial shading

1. Introduction

Harvesting solar energy is efficient and sustainable, presenting a possible solution to the global energy crisis. The global solar capacity reached 400 GW by the end of 2017. The deployment of photovoltaic (PV) generation with additional capacity of 50 GW, 10 GW, and 8 GW in China, the USA, and India, respectively, was an extraordinary record in 2017. The decreasing cost of PV panels and the availability of controllable power electronic converters have led to huge worldwide growth in off-grid and grid-connected PV systems for reliable power utilization [1,2]. In PV systems, maximum power point tracking (MPPT) methods such as perturb and observe (P&O) and incremental conductance [3] can be implemented to track the optimal operating point. However, they suffer from the steady-state oscillations that occur around the peak and failure during rapid change in insolation, which reduces the efficiency of the PV system [4]. The output of a PV array declines when some of the modules are shaded by some obstacles such as tree branches, buildings, moving clouds, pole structures, and dust deposition. The decline in current output from a partially shaded array is proportional to the portion of the module that is obscured and the opacity of the obscuring objects. Under partial shading conditions (PSCs), the P-V characteristics have several peaks, one of which is the global maximum operating

*Correspondence: chansekaran23@gmail.com

This work is licensed under a Creative Commons Attribution 4.0 International License.

point (GMOP), the others being local maximum operating points (LMOPs) [5]. Application of conventional MPPT techniques under such conditions leads the PV panel to operate at any one of the local power peaks with reduced efficiency [6]. During PSCs, special techniques need to be employed to detect partial shading and provide the necessary duty cycle to the converter. One of the works on partial shading of PV systems reported an efficient manner by which PSCs can be detected and how the global maximum power point (GMPP) can be tracked [7]. A comparative analysis between different MPPT techniques employed for PV panels during nonuniform irradiance can be found in [8–11]. A bioinspired algorithm-based MPPT employed for PSC was elaborated in [12]. A modified beta algorithm and PSO-based tracking of the GMPP was discussed in [13,14]. These soft computing techniques find applications in MPPT due to their ability to solve the nonlinear P-V function during PSCs. The performance of these methods varies in different aspects such as convergence speed, complexity in tuning the parameters, steady-state performance, cost, and capability to detect the GMOP under different irradiance patterns. Recently, a metaheuristic algorithm known as the firefly (FF) algorithm was developed [15], inspired by the social behavior of fireflies. In addition to our previous work, several works on the FF algorithm have been published [15]. Following the interest in this algorithm, this paper transforms the FF method for designing an intelligent MPPT scheme to determine GMOP, maintaining inheritance of firefly behavior while adding fast convergence properties. In this context, the fast convergence firefly algorithm is proposed to track the GMOP under normal irradiance and in various PSCs of PV systems, which improves all the performance aspects in real time. The remainder of the paper is organized as follows. Section 2 introduces the optimization problem formulation for MPPT with duty cycle as the solution. Section 3 presents the description of the conventional firefly algorithm. Section 4 discusses the need for the FCFA and also presents a description of the proposed MPPT method. Section 5 verifies the proposed method through simulation and experimental results. Finally, the conclusion is reported in Section 6.

2. Problem formulation

The block diagram for tracking the GMOP under PSCs by controlling a DC-DC converter connected to the PV array is shown in Figure 1. The main objective of the problem is to track the GMOP under different irradiance conditions by operating the converter at optimal duty cycle (d).

The problem formulation for MPPT is as follows:

$$Maximize\ P_{pv}(d), \tag{1}$$

$$Subject\ to\ d_{min} \leq d \leq d_{max}, \tag{2}$$

where P_{pv} is the output power of the PV panel; d_{min} and d_{max} are respectively the minimum and maximum values of the duty ratio, taken to be 10% and 90%, respectively; and d is the duty ratio of the boost converter.

3. Firefly algorithm

A metaheuristic algorithm developed by Yang known as the firefly algorithm (FA) has been successfully implemented for different benchmark functions [10]. The algorithm's performance and the superiority of the FA have been verified and confirmed [11]. A firefly's position, x_i, is updated using Eq. (3):

$$x_i^{(k+1)} = x_i^{(k)} + \beta(r) \times (x_i^{(k)} - x_j^{(k)}) + \alpha(rand - \frac{1}{2}), \tag{3}$$

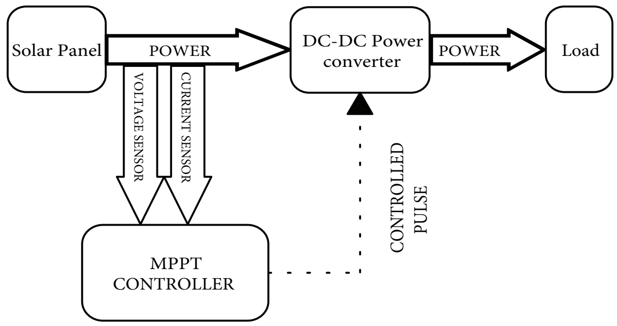

Figure 1. Block diagram for MPPT.

where $x_i^{(k)}$ and $x_j^{(k)}$ are the current positions of the fireflies at the kth iteration. The second term in Eq. (3) is an attractiveness function, β, and is calculated using generalized Eq. (4):

$$\beta(r) = \beta_0 e^{-\gamma r^n}. \tag{4}$$

γ is an absorption coefficient, which controls variation in attractiveness. β_0 is the initial attractiveness and n is a constant value between 0 and 2. The distance between two fireflies r_{ij} is represented as Euclidean distance, calculated using Eq. (5):

$$r_{ij} = \|x_i - x_j\| = \sqrt{\sum_{q=1}^{D}(x_{i,q} - x_{j,q})^2}. \tag{5}$$

The third term in Eq. (3) is a randomization factor, where α is constant. For each movement of a firefly, 'rand' is a randomly generated number, the value of which is uniformly distributed between 0 and 1.

4. Proposed fast convergence firefly algorithm (FCFA)

For the conventional FA, the second term in Eq. (3) depends entirely on the distance between two fireflies, raising a potential problem for the algorithm as applied to the MPPT system. For discussion of this problem, a three series and two parallel PV array termed "3s2p configuration" with one distinct insolation pattern is imposed and the PV power with corresponding duty ratio is computed and plotted in Figure 2a.

The four fireflies considered in this analysis (F1, F2, F3, and F4) are initially distributed uniformly across the solution space at a 30% interval as shown in Figure 2a, where F1, F2, F3, and F4 are marked respectively with a square, circle, star, and triangle. Their respective duty cycles are calculated during an iterative process, with each attracted by the brightest firefly. Considering firefly F1, it will modify its position based on a randomly selected neighboring firefly. If F1 updates its position with respect to the randomly selected F2, because F2 is brighter than F1 (i.e. the power corresponding to the duty cycle of F2 is greater than that of F1), F1 will move towards F2. The probability of moving beyond F2 is zero, as shown in Figure 2b. This scenario may take several iterations to reach the maximum value. On the other hand, if firefly F1 updates its position with respect to the randomly selected F4, F1 will move towards F4 instead. Changes that are too large may lead the fireflies to escape from the vicinity of the global point, as shown in Figure 2c. The same scenario will occur when the GMOP is located on the right side and LMOP is located on the left of the curve. Second, with increasing iterations, the distances between any two fireflies will reduce since they move towards a brighter firefly as shown in Figures 2b and 2c. Due to this characteristic of the FA, the exponential term in Eq. (4) will

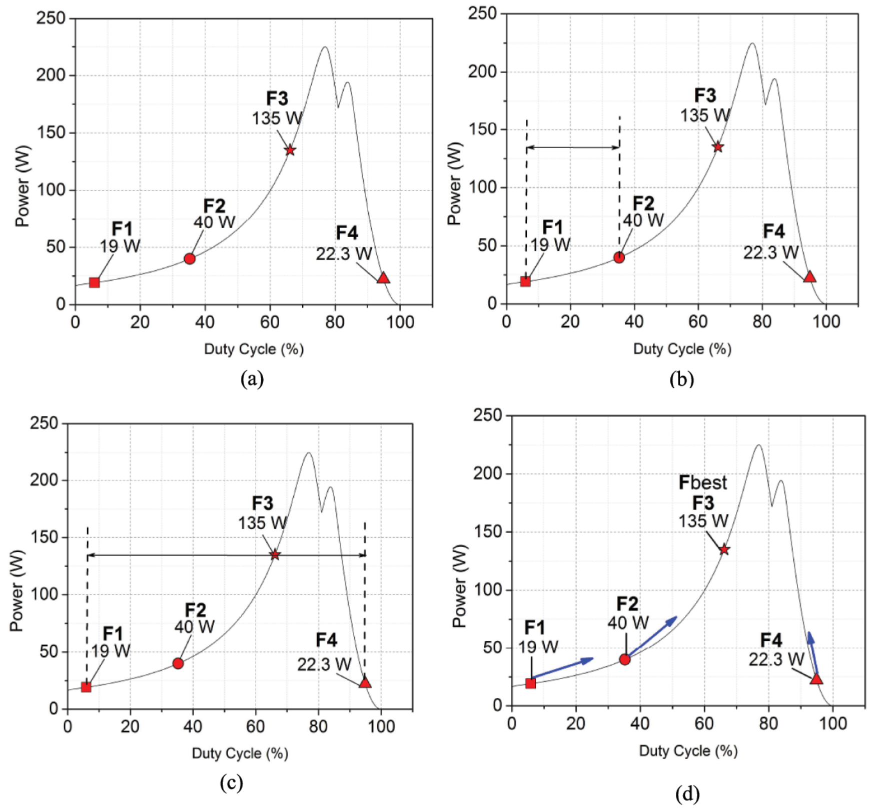

Figure 2. Firefly-based GMOP tracking behavior.

increase with further iterations, which again leads the fireflies to escape from the vicinity of the global point. The randomization factor in the third term in Eq. (3) presents a further problem. In the application of MPPT, the firefly will be directed towards brighter fireflies (i.e. maximum power) as shown in Figure 2d.

A firefly's direction of movement is partially determined by the term ($rand\frac{1}{2}$). If the generated random number is less than 0.5, the third term will be negative. On the other hand, if the generated random number is greater than 0.5 then the third term will be positive. The distance moved in that direction is controlled by the value of randomization factor α, which has a standard value for randomization between 0 and 1. That standard value greatly reduces the contribution of the factor α to fireflies' changes in position. The above problems are solved by considering the nature of P-V curves under partial shading and considering advantages of FA properties as described in Section 3. Removing the random third term, $\alpha rand\frac{1}{2}$, the second term may be modified for MPPT application by taking advantage of firefly characteristics, transforming the conventional FA into a fast convergence structure. The modified firefly equation is given in Eq. (6) as follows:

$$x_i^{(k+1)} = x_i^{(k)} + \beta(k) \times (F_{best}^k - x_i^{(k)}), \tag{6}$$

where x_i^k is the current position of the fireflies at the kth iteration and F_{best}^k is the brightest firefly position at the kth iteration.

Consider the same pattern as before, with F1, F2, F3, and F4 the initial positions of the fireflies. Among the four fireflies, F3 is the brightest firefly position, F_{best}, as shown in Figure 3a. With the proposed modification, the remaining fireflies (F1, F2, and F4) will move towards the F_{best} position, reaching a global point. Since F3 is the brightest firefly, the duty cycle of F3 is unchanged, and F3 does not contribute to the exploratory process. To avoid this, a small perturbation is introduced to ensure changes in power towards global maxima, reducing the chance of missing the global peak. Similarly, the attraction function β is determined for the application of MPPT to be a monotonically decreasing function. The proposed second term decreases exponentially as the iteration progresses, as shown in Eq. (7):

$$\beta(k) = \beta_0 e^{-\gamma(\frac{k}{k_{max}})}, \tag{7}$$

where k is the iteration number and k_{max} is the maximum number of iterations. β_0 is an initial attractiveness value fixed as 1. Initially, the change in step is large; with further iterations, the step level is reduced due to the exponential term, accurately tracking the global point with fewer iterations. Even with different values of β_0 and γ between 0 and 1, it will not affect the solution quality and convergence speed since it depends on the $\frac{k}{kmax}$ and $(F^k_{best} - x^k_i)$ terms. Hence, the tuning of FCFA parameters is eliminated in the proposed method. The movement of firefly F1 with respect to the global point is shown in Figure 3b. The flowchart of the proposed method is given in Figure 4.

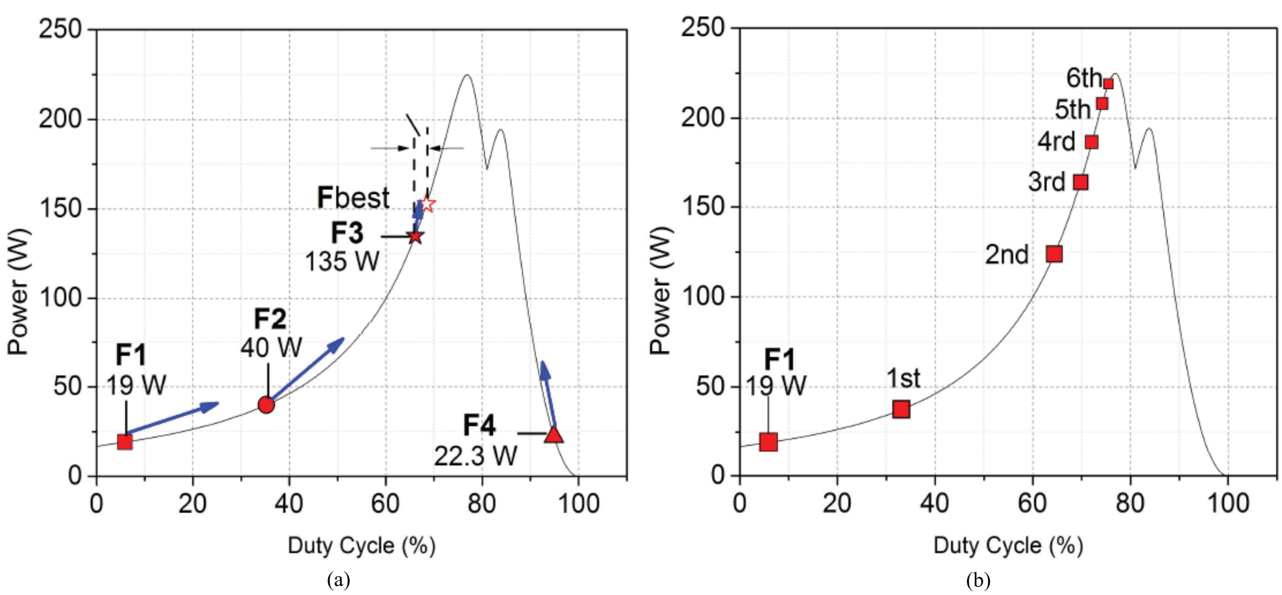

Figure 3. FCFA-based GMOP tracking behavior.

5. Results and discussion

5.1. PV array configuration

An equivalent circuit of a single solar-cell model implemented in the literature [16] is employed in MATLAB simulations. The simulation considers three series and two parallel PV modules, called a 3s2p configuration, as shown in Figure 5a, with each module rated 50 W and the total rating of PV system 300 W. The blocking diodes are connected in series with a string to prevent reverse current flow. The presence of bypass diodes in each PV module within a string prevents hot spots but introduces multiple peaks in the P-V curve under PSCs. Here, four different insolation patterns are considered for the above configuration, as shown in Table 1. Under

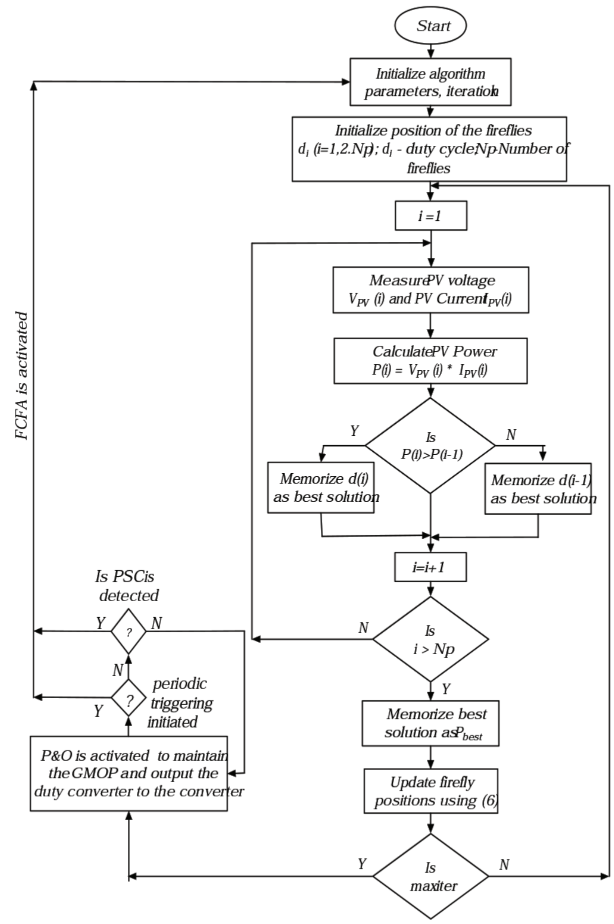

Figure 4. Flowchart to track GMOP using FA.

each pattern (1 to 4), the variation of irradiance for different curves (A to D) is given in Table 1. Based on this irradiance, the four curves obtained for each pattern are shown in Figure 5b. Irradiance of the PV array is varied for every 30 s (t_{max}) in MATLAB simulations; therefore, a complete test of all four patterns requires 120 s.

5.2. Simulation results

Variations in PV output power and the duty ratio of the DC-DC converter are computed [16] for the different patterns in Figure 5b, with the results shown in Figure 6. The partial detection method is adapted from [14] to detect PSCs. If PSC is detected then the standard PSO, FA-based MPPT algorithms, and proposed FCFA are employed in MATLAB to track the GMOP for four patterns. In the partial shading detection presented in [14], if the measured operating voltage and current do not indicate any disturbance during pattern changes, then the algorithm cannot detect this situation. In this situation, especially in changing partial shading patterns, no big change in the array power is observed. Therefore, periodical triggering is also incorporated in the paper to handle these situations [17] and a suitable time interval should be selected. The time interval between two consecutive triggers has to be decided based on the settling time of the converter and climatic conditions of the PV array location. Therefore, the time interval between two consecutive triggers should be greater than the settling time of the converter to avoid energy loss, which affects the efficiency of the system. In addition, the

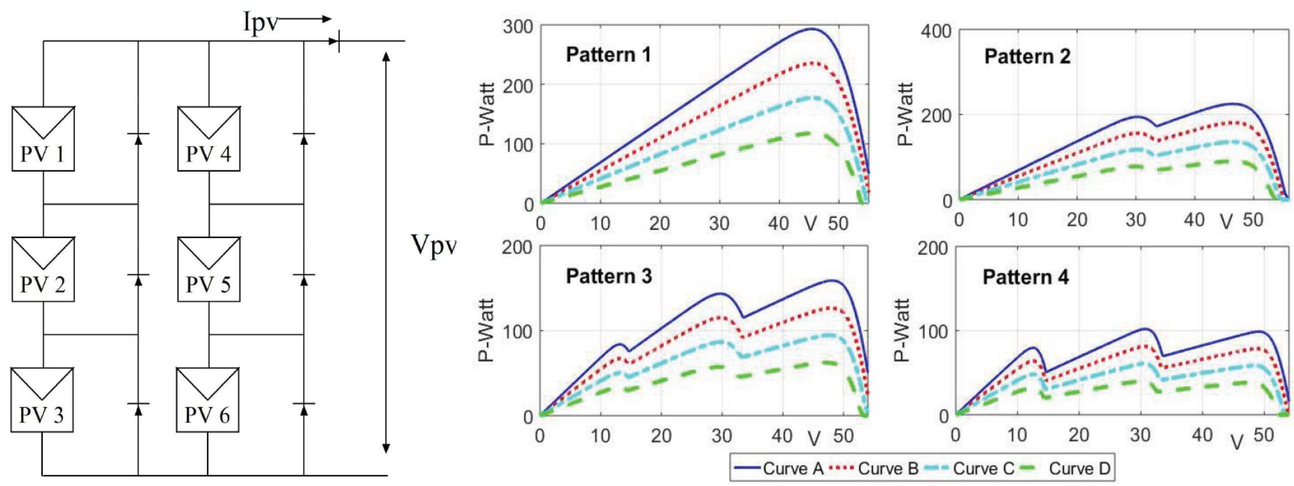

(a) (b)

Figure 5. (a) PV array configuration, (b) P-V characteristics under varying insolations.

Table 1. Pattern design.

Pattern number	Module number	Curve A	Curve B	Curve C	Curve D	Pattern number	Module number	Curve A	Curve B	Curve C	Curve D
Pattern 1	PV1	1000	800	600	400	Pattern 3	PV1	1000	800	600	400
	PV2	1000	800	600	400		PV2	500	400	300	200
	PV3	1000	800	600	400		PV3	500	400	300	200
	PV4	1000	800	600	400		PV4	1000	800	600	400
	PV5	1000	800	600	400		PV5	1000	800	600	400
	PV6	1000	800	600	400		PV6	500	400	300	200
Pattern 2	PV1	1000	800	600	400	Pattern 4	PV1	1000	800	600	400
	PV2	1000	800	600	400		PV2	500	400	300	200
	PV3	500	400	300	200		PV3	300	240	180	120
	PV4	1000	800	600	400		PV4	1000	800	600	400
	PV5	1000	800	600	400		PV5	500	400	300	200
	PV6	1000	800	600	400		PV6	300	240	180	120

interval time has to be decided based on the climatic condition of the PV array location (i.e. history of data of irradiance level variation in the previous years). In all three algorithm, once the GMOP is tracked, the P&O algorithm is initiated with small steps to maintain the GMOP further for any change in irradiance value. To obtain accurate MPP tracking larger numbers of particles are required. However, it takes more computation time. Therefore, a trade-off should be made to ensure good tracking speed and accuracy. The obtained best number of particles is four and these particles are initially distributed uniformly across the solution space at a 30% interval. Hence, whenever tracking is triggered, the particles are set to the initial position. Also, the constants of PSO and FA parameters are determined using sensitivity analysis. Let us discuss the MPPT variation with respect to the PSO constants (initial values). The PSO algorithm control parameters are w, c1, and c2. Here, parameter w is fixed and the other parameters, c1 and c2, are varied from 0.1 to 1 with a step interval of 0.1. Pattern 2 (maximum irradiance - blue curve) is considered for simulation and results for different parameters are given in Table 2.

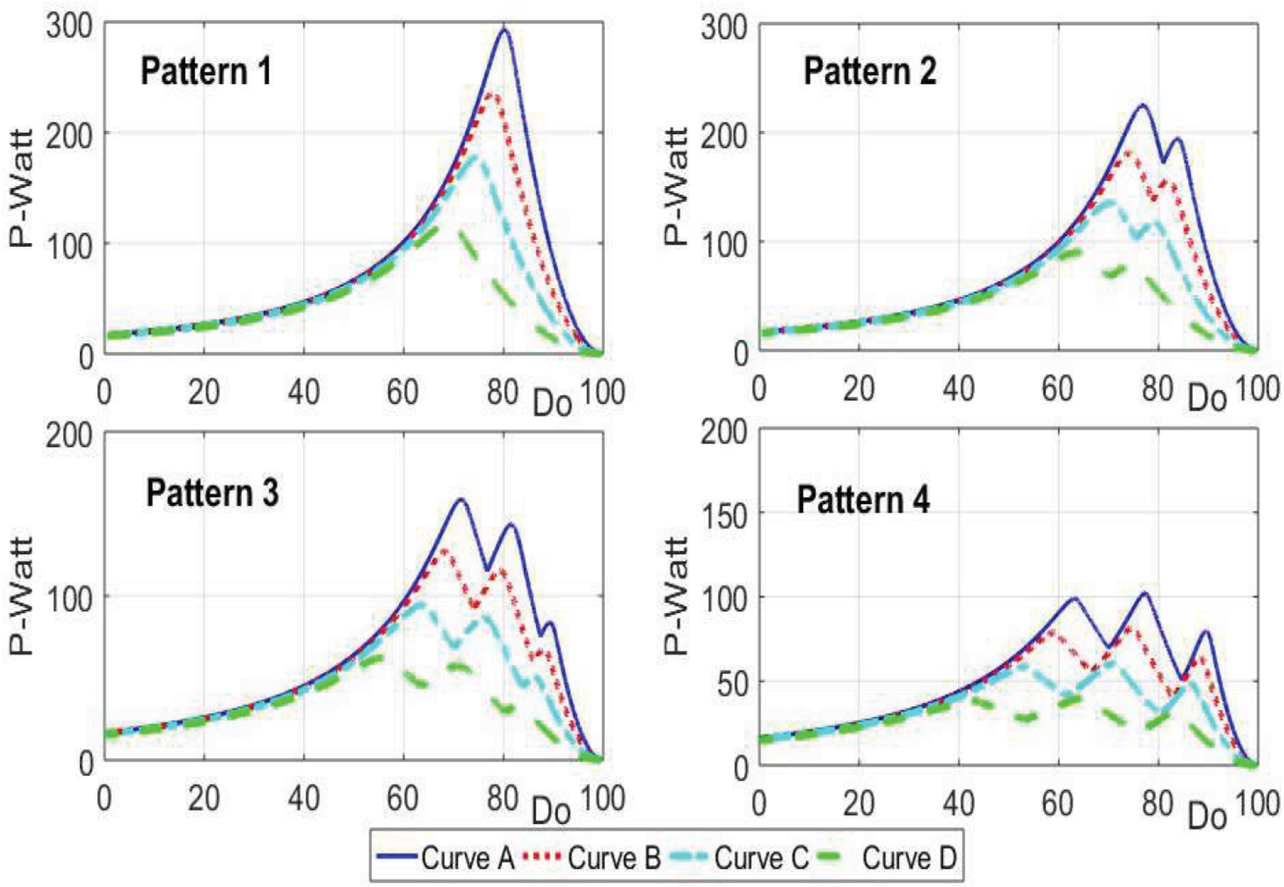

Figure 6. PV o/p power and duty ratio of the DC-DC converter.

From Table 2 it is observed that the accuracy and computational time are good only in a certain region of the parameter, which is shown with gray shading in Table 2. Hence, the best parameters for PSO are considered as w = 0.5, c1 = 0.5, and c2 = 0.4. Also, the best parameter is tested with different irradiance and it is found that these parameters determine the best solution. Similarly, the best parameters for FA and FCFA are given in Table 3. With the above PSO and FA parameters, simulations are executed for four different patterns.

The main advantage of the proposed method is that it completely eliminates the parameter tuning requirements in soft computing techniques. The value of β_0 and γ is set to 1 since it will not affect the solution quality and convergence speed. Here, for every 30 s the pattern is varied in the MATLAB code and computed results are shown in Figure 7. With the above PSO, FA, and FCFA parameters, the simulation is executed for four different patterns. The PSO, FA-based MPPT, and FCFA methods' tracking consistently identifies the GMOP and near-GMOP in all four patterns. From Figure 7, it is observed that the PSO, FA, and FCFA are successfully capturing GMOPs in partially shaded PV systems. From Figure 7a, when using PSO it is found that there are more oscillations in the initial stages of tracking; the oscillation drastically reduces as the search proceeds. Also, the power curve oscillations shown in Figure 7b are less when tracking with the FA compared to PSO. The FCFA is employed to track the GMOP for the four patterns shown in Figure 7c. From the results, it

Table 2. Parameter setting analysis.

	c2	c1									
		0.1	0.2	0.3	0.4	0.5	0.6	0.7	0.8	0.9	1
P (W)	0.1	287.5	286.4	290.5	292.23	292.54	291	290.31	290.2	289.01	290
Time (s)		12.11	12.14	12.10	10.12	10.10	11.01	12.85	11.89	12.15	12.01
P (W)	0.2	290.5	290.3	290.1	292.9	292.34	290.00	290.97	290.03	289.00	290.00
Time (s)		12.15	12.15	12.00	10.45	10.97	12.10	12.81	12.01	12.14	12.10
P (W)	0.3	288.3	290.1	290.31	292.88	292.03	291.5	289.87	290.31	290.31	290.70
Time (s)		12.11	12.14	12.9	10.7	10.12	12.33	12.81	12.9	12.77	12.01
P (W)	0.4	290.5	290.3	290.97	292.9	292.9	290.11	290.11	290.97	290.97	290.00
Time (s)		12.13	12.13	12.83	10.12	10.10	11.61	12.70	12.83	12.83	12.10
P (W)	0.5	290.01	291.5	290.11	292.9	292.89	290.32	287.5	290.11	291.5	290.11
Time (s)		12.11	12.31	12.70	10.11	10.08	12.87	12.11	12.70	12.31	12.70
P (W)	0.6	290.9	289.87	289.82	292.9	292.89	291.4	290.5	288.3	290.11	288.09
Time (s)		12.87	12.81	12.51	10.99	11.01	12.30	12.99	12.11	12.60	12.58
P (W)	0.7	291.9	290.11	289.87	291.78	291.99	290.03	290.97	290.5	291.5	290.5
Time (s)		12.91	12.70	12.81	11.08	12.85	11.01	12.92	12.13	12.34	12.10
P (W)	0.8	290.11	289.81	290.17	291	291.31	290.11	290.69	287.01	290.11	290.69
Time (s)		12.67	12.40	12.64	11.21	12.03	11.99	12.70	12.19	12.60	12.71
P (W)	0.9	290.01	289.87	289.01	291.03	291.31	289.5	289.72	288.9	291.5	290.9
Time (s)		12.11	12.81	12.15	11.08	12.85	12.11	12.51	12.57	12.34	12.87
P (W)	1	290.11	290.11	289.00	291	291.31	290.11	288.87	285.9	290.11	291.9
Time (s)		12.67	12.70	12.59	11.01	12.85	11.67	12.81	12.91	12.60	12.90

Table 3. Algorithm parameters.

PSO algorithm		Firefly algorithm		FCFA method	
Parameter	Values	Parameter	Values	Parameter	Values
w	0.5	γ	0.8	β_0	1
c1	0.5	β_0	1.5	γ	1
c2	0.4	α	0.45	Firefly size	4
Particle size	2	n	0.5		
		Firefly size	4		

is found that FCFA is superior to the other algorithms available in the literature and eliminates the parameter tuning requirements. Furthermore, the proposed method is validated by changing the irradiation among the patterns (i.e. switching the irradiation patterns from 1 to 4 and back to 1), as shown in Figure 8. Here the simulation is carried out for 150 s. For every 30 s, pattern 1-curve A, pattern 2-curve B, pattern 3-curve C, pattern 4-curve D, and again pattern 1-curve A from Figure 5b are simulated and the results are presented in Figure 9. From the results, it is found that FCFA is superior to other algorithms available in the literature.

In order to strengthen this argument and prove the above statement, the proposed method is implemented for different configurations of the PV array and the simulation results are presented in Table 4. Here the efficiency

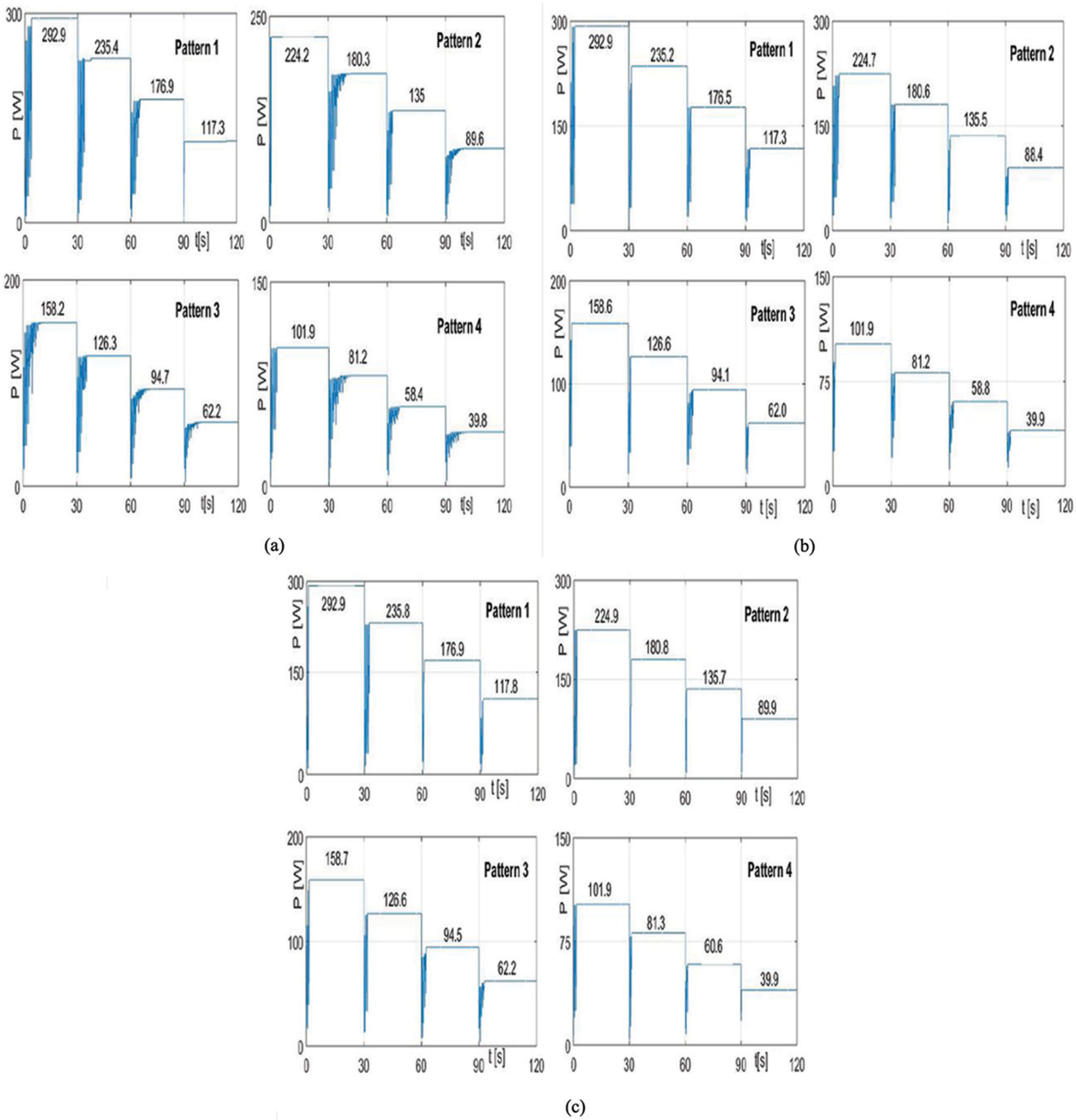

Figure 7. GMOP curves for 3s2p configuration - dynamic response: (a) PSO, (b) FA, (c) FCFA.

(μ) of each method is calculated [18] using Eq. (8):

$$\mu = \frac{Energy\ extracted\ by\ a\ given\ MPPT\ scheme\ during\ t_{max}}{Maximum\ energy\ available\ during\ t_{max}}. \tag{8}$$

From the above discussion, it is concluded that the proposed FCFA tracks the maximum power for any PV configuration without any parameter tuning.

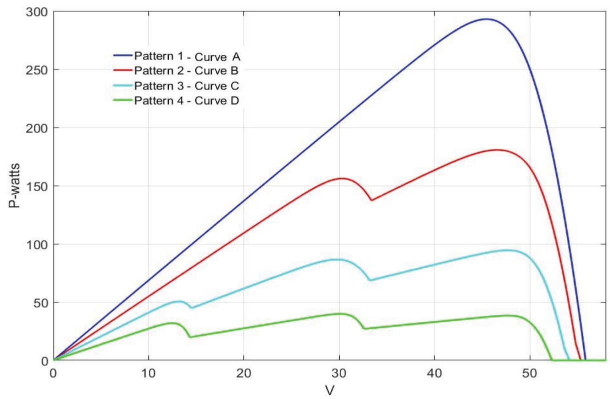

Figure 8. PV curve with different patterns for simulation study.

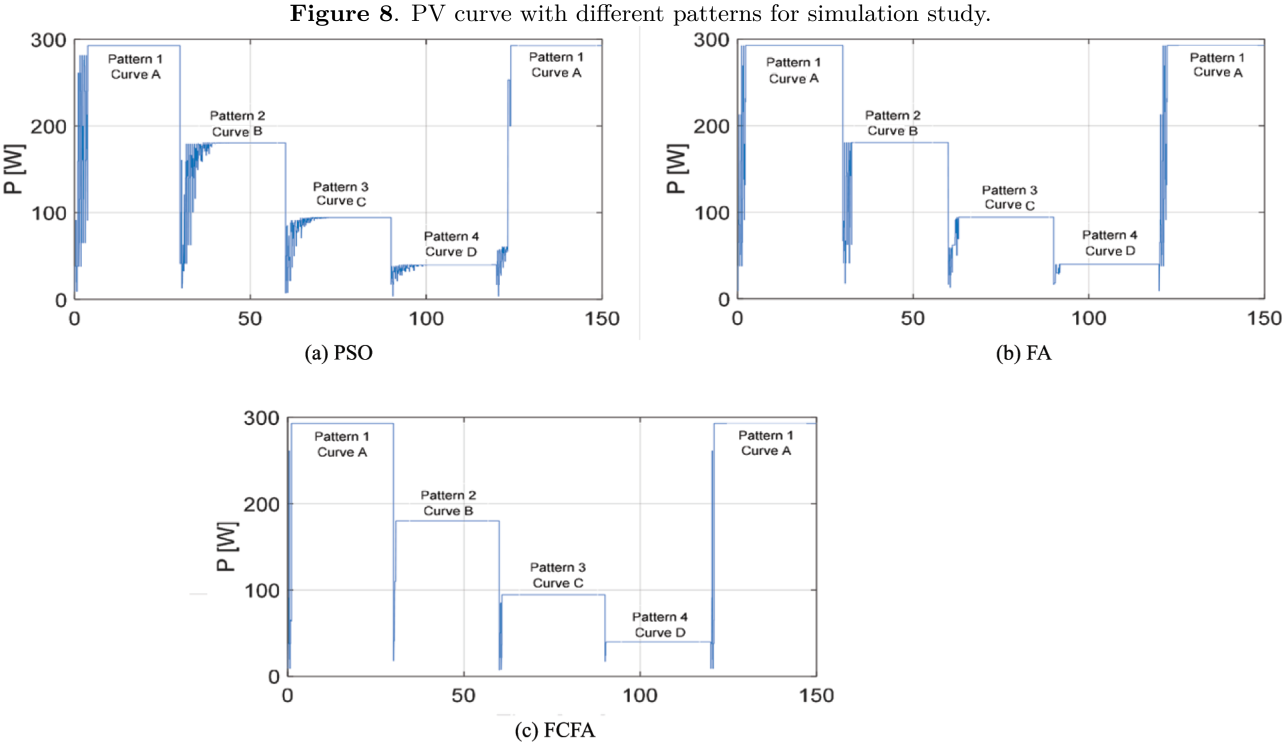

Figure 9. Simulation results for different patterns.

5.3. Experimental results

The FCFA is verified with a 300-W PV system with the 3s2p configuration. To create PSCs, opaque sheets are positioned on the PV panel. Figure 10 shows the block diagram of the hardware setup operated with switching frequency of 20 kHz. The specifications of the PV module are given in Table 5.

In Figure 10, the PV current and voltage are sensed using a sensor (HE055T01) and transducer (LV25-P). The sensed analog PV output parameters are converted to digital values for computation using 12-bit ADC with sampling rate of 1 MSPS. A Xilinx Spartan-6 FPGA is used as a controller device to implement the MPPT algorithms. The MPPT algorithm is developed using different algorithms (duty sweep, FA, PSO, FCFA) and tested using the ISE 14.7 of XILINX. The standard PSO and FA-based MPPT algorithm are implemented in the FPGA and similar to Section 5.2 the parameters are tuned. The best parameters for PSO and FA are

Table 4. PV power for different PV configurations.

PV configuration	Maximum power tracking achieved in watts			Average efficiency in %	Average tracking time (s)
	Pattern 1 Curve A 1000 W/m^2	Pattern 1 Curve B 800 W/m^2	Pattern 1 Curve C 600 W/m^2		
3s2p	360	288	216	99.83	1.212
5s2p	600	480	360	99.84	1.226
10s5p	3000	2400	1800	99.81	1.278
3s	180	144	108	99.76	1.220
5s	300	240	180	99.83	1.201
10s	600	480	360	99.84	1.273

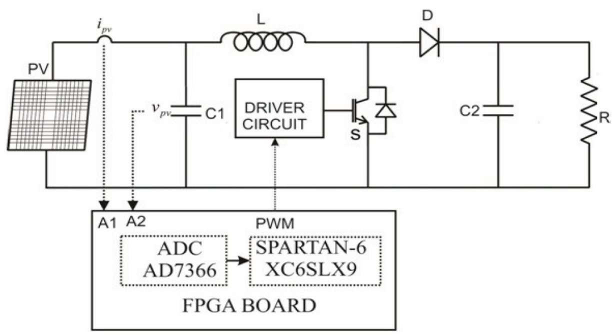

Figure 10. Block diagram of experimental setup.

Table 5. PV module specifications.

PV module	
Peak power	50 W
Maximum voltage	18.54 V
Open circuit voltage	22.68 V
Maximum current	2.7 A
Short circuit current	2.97 A

tabulated in Table 6. The FCFA performance is tested under the following patterns, which is shown in Figure 11:

a) Pattern A: Uniform irradiance in all PV panel.

b) Pattern B: One of the PV panels in a series string is heavily shaded.

c) Pattern C: One of the PV panels is lightly shaded.

Figure 12 compares the proposed FCFA with the duty sweep method, standard PSO, and the firefly algorithm for these three shading patterns. In the duty sweep method, to scan the entire PV curve, the duty cycle is varied from maximum to minimum value, and the method is initiated at the trigger point shown in Figure 12a. The trigger point is the same for the other algorithms. The three different measured PV patterns are indicated in Figure 12a as patterns 1, 2, and 3. On observing the curve, pattern 1 has one peak curve and two peaks are found in patterns 2 and 3 at different times, represented by the dotted circle in Figure 12a.

Figure 11. PV pattern for experimental setup.

Table 6. Algorithm parameters - experimental results.

PSO		FA	
No. of populations	4	No. of populations	4
w	0.5	β_0	1
c1	0.5	γ	2
c2	0.4	α	0.45

After scanning, the duty cycle with respect to GMOP is fed to the converter through the PWM generator to make the PC array operate at GMOP, after which the P&O method is implemented for further maximum power tracking. The duty sweep method has high tracking accuracy, since the method scans the entire PV curve. The average tracking time of the duty sweep method is 2.7 s. The variations in PV current and voltage with respect to maximum power are also shown separately for each pattern in Figure 12a. Similarly, Figure 12b shows the tracking behavior of PSO for the three patterns. Tracking accuracy is good with much better tracking speed than the duty sweep method due to optimistic search. Before triggering, the maximum output power is 101 W (pattern 2). After triggering, the operating point shifted to 108 W. The tracking time of PSO is 2.5 s. The tracking behavior of the FA for patterns 1 through 3 is shown in Figure 12c. Based on simulated and experimental results, the FA is faster than PSO due to the tracking nature of the FA. Finally, the FCFA method is implemented to track the GMOP for the three patterns, with results shown in Figure 12d. Clearly, the proposed FCFA identifies the GMOP faster than the duty sweep method, PSO, and FA. Figure 12 shows that the duty sweep method, PSO, the FA, and the proposed firefly methods are well suited to tracking the GMOP under uniform and partial shading conditions; however, the proposed FCFA is faster than the other three methods, which in turn improves the overall efficiency of the tracking system. Also, the FCFA technique greatly reduces turbulence. The FCFA shows better results than the other methods, tracking the GMOP the fastest and taking 1.2 s for all tested shading samples.

5.3.1. Load disturbance

To illustrate the effectiveness of the proposed method a strong load fluctuation is introduced to shift the operating point from the GMOP to one of the LMOPs as shown in Figure 13. The duty sweep method, PSO, FA, and proposed FCFA are successful in tracking the GMOP. The tracking time of proposed method is less than that of the other methods.

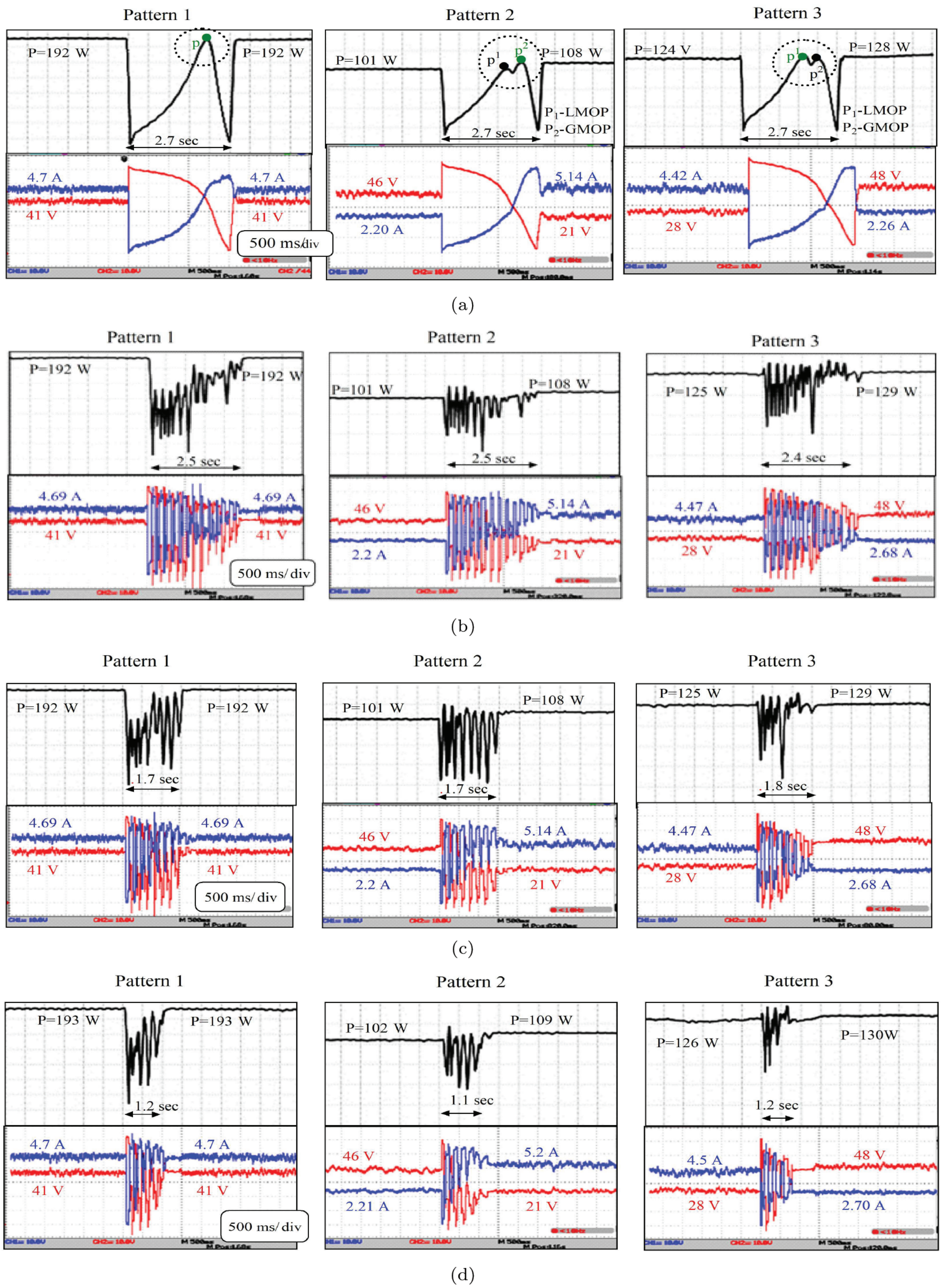

Figure 12. Experimental results for (a) duty sweep, (b) PSO, (c) FA, and (d) FCFA method.

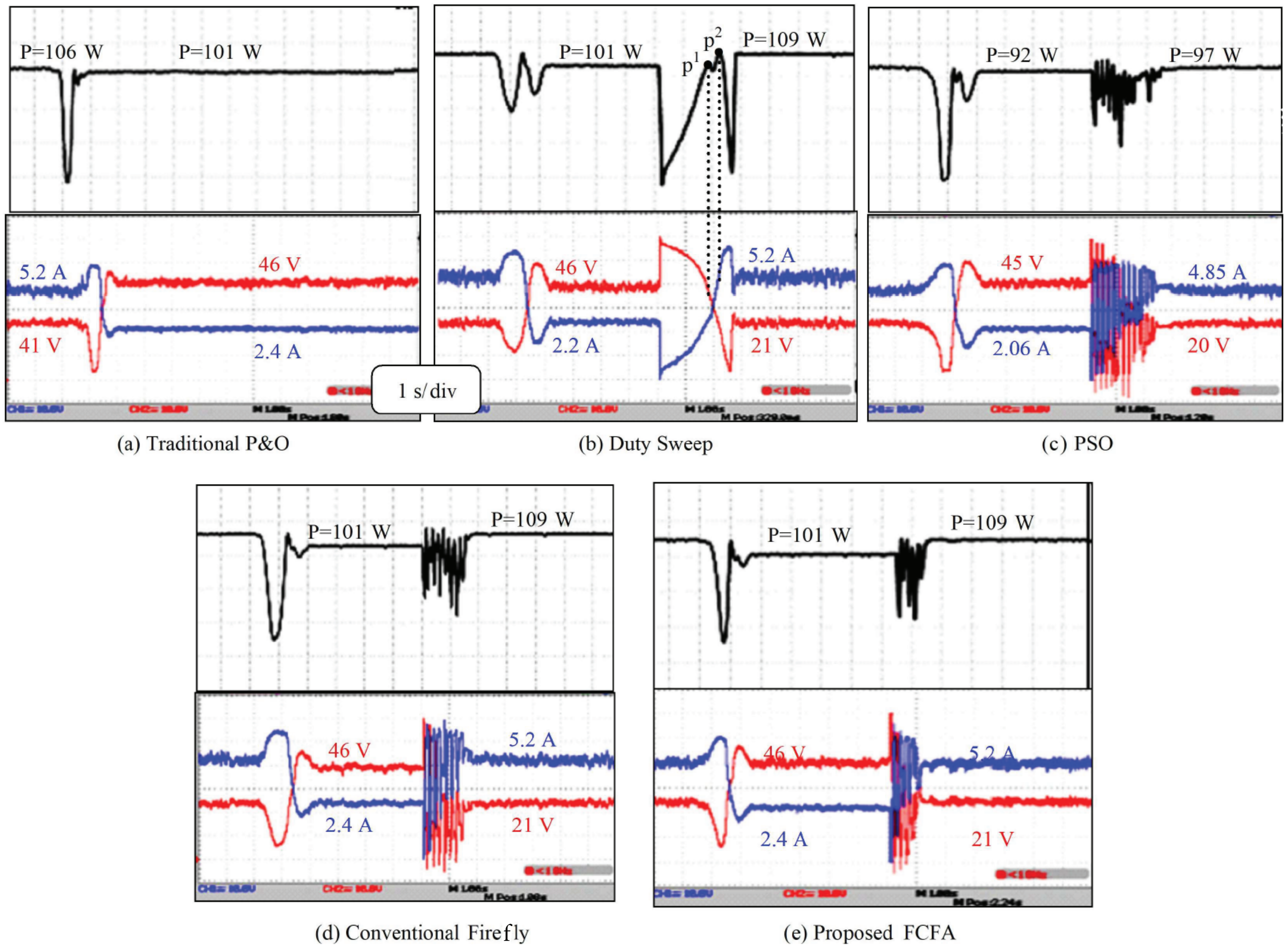

Figure 13. Load disturbance.

5.3.2. Performance analysis

To study the superiority of the proposed FCFA method, parameters such as tracking time and converged iteration are considered. The comparison of results with the algorithms existing in the literature is shown in Table 7. From Table 7, it is found that the proposed method takes 1.2 s and 5 iterations to converge to the global maximum power, which shows the superiority of the proposed method. Although the OD-PSO has taken fewer iterations to converge than the FCFA, the computation of OD-PSO takes slightly more time per iteration. Also, to validate the proposed FCFA with the conventional method, the tracking time of the FCFA is compared with the conventional method adapted from [7]. This conventional method takes less time compared with the proposed method. This method is faster for PSCs with fewer peaks. However, if the number of peaks is larger the GMOP tracking will be slower, due to the tracking of all the local peaks one by one for comparison.

In order to strengthen this argument and prove the benefits of reduced convergence time, the proposed method is validated on a grid-connected 5-kW solar power plant at NIT Puducherry, Karaikal, India, which was commissioned under the CPRI Project Fund in 2017-2019. The hardware setup is shown in Figure 14.

The performance of the proposed algorithm is tested under PSCs. Now PSO, FA, and FCFA methods are employed to track maximum power. Figure 15 shows the convergence time taken by each algorithm to reach

Table 7. Comparison of results.

Sl. no.	Solution techniques	Operates both PSC and uniform	Tracking time (s)	Converged iteration
1	PSO [16]	Yes	11.5	-
2	ACO [16]	Yes	8.5	-
3	P&O [16]	No	12	-
4	ACO-P&O [16]	Yes	3.5	-
5	PSO [19]	Yes	5.90	27
6	Jaya [19]	Yes	3.47	16
7	GRP-Jaya [19]	Yes	1.90	9
8	Modified I&C [13]	No	9	-
9	Technique [13]	Yes	7.5	-
10	Modified beta algorithm [13]	Yes	4.5	-
11	Hybrid algorithm [14]	Yes	3.85	3
12	Extension P&O method [20]	No	2.5	-
13	Conventional P&O [20]	No	5	-
14	Variable step P&O [20]	No	4	-
15	OD-PSO [21]	2.08	Yes	4
16	Firefly algorithm [21]	Yes	2.21	5
17	Hybrid PSO-P&O [21]	Yes	2.74	7
18	Analytical method [22]	Yes	2.5	-
19	PSO	Yes	2.4	7
20	FA	Yes	1.7	7
21	FCFA	Yes	1.2	5

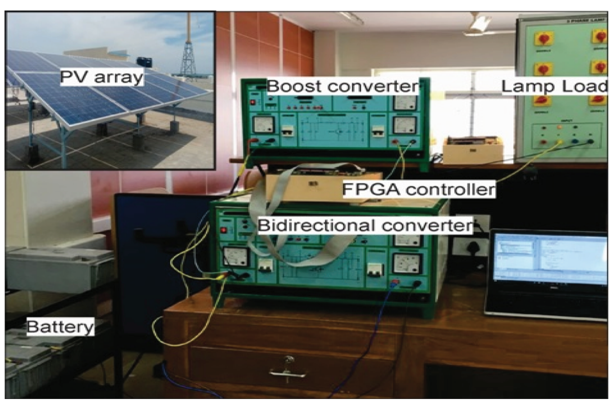

Figure 14. Hardware setup of 5-kW solar plant.

the maximum available power. This figure again validates the effectiveness of the proposed algorithm, which has the least convergence time. Since the tracking time of the FCFA is less than the others, the FCFA generates more income by extracting higher energy from the PV arrays. An overall performance comparison is given in Table 8. Thus, from Figure 15 and from Table 8, it can be concluded that the proposed algorithm enhances the performance of the PV plant in real time.

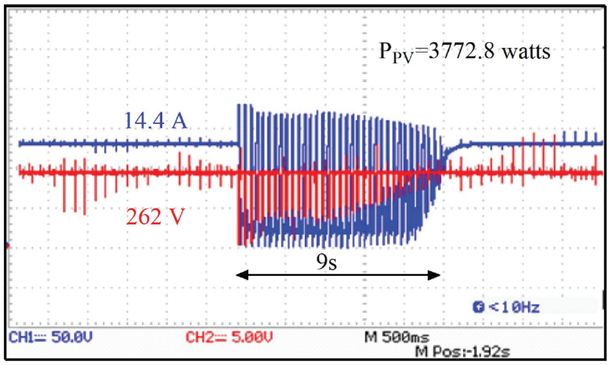

(a)

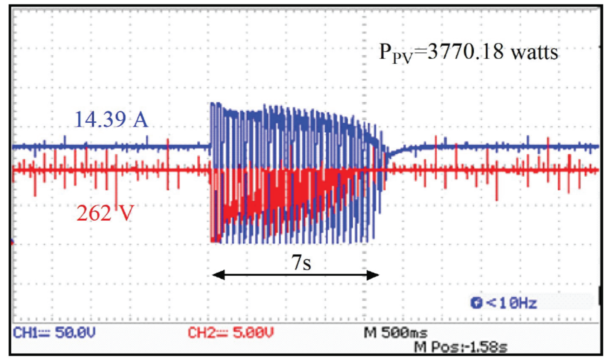

(b)

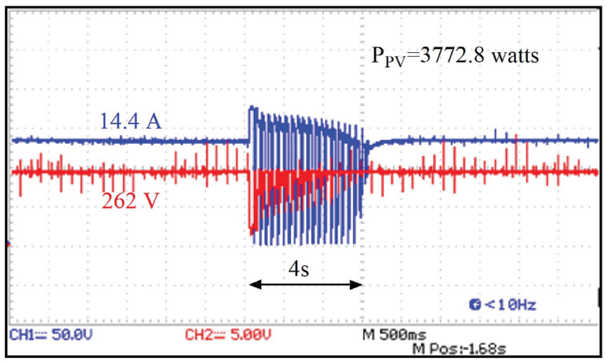

(c)

Figure 15. Convergence time - 5-kW solar plant: (a) PSO, (b) FA, (c) FCFA method.

Table 8. Performance comparison.

Sl. no.	MPPT methods	Simulation aspects			Hardware aspects			
		Tracking speed	Suitability under partial shading	Parameters tuning	Level of complexity	Efficiency	System cost	Convergence time
1	P&O	Low	NO	Not required	Low	Low	Low	Medium
2	Duty sweep	Low	Yes	Not Required	Medium	High	Medium	Medium
3	PSO	Medium	Yes	Required	Medium	High	Medium	Low
4	FA	Medium	Yes	Required	Medium	High	Medium	Low
5	FCFA	High	Yes	Not required	Medium	Very high	Medium	Very low

6. Conclusion

This paper has presented FCFA, a new MPPT algorithm based on firefly behavior, for fast tracking of the GMOP of partially shaded PV arrays. The FCFA simplifies the control structure of MPPT by removing the random factor and modifying the attractive nature of fireflies from the standard FA. Also, the proposed FCFA method completely eliminates the parameter tuning requirements. These are the major deviations from the traditional FA. The fireflies begin their search positioned at possible solutions within the search space. Based on the proposed FCFA behavior, the fireflies move to the GMOP. The suitability of this algorithm for MPPT is logically proven and the results are analyzed. Simulations using four different shading patterns and four different insolations demonstrated that the FCFA is system-independent and quickly converges to the GMOP. Similarly, experiments performed with two different PV configurations have demonstrated that the FCFA quickly converges to the GMOP, outperforming existing methods such as the duty sweep method, standard PSO, and FA in terms of tracking speed and accuracy.

Acknowledgments

This research work was funded and supported by the Central Power Research Institute (CPRI), Ministry of Power, Government of India, Bangalore (RSOP/2015/DG/8/15122015). This research work was also supported by the Ministry of Electronics and Information Technology, Government of India, under the Visvesvaraya PhD Scheme.

References

[1] Leo R, Milton S, Senthilkumaran M. Implementation of energy management and demand side management of a solar microgrid using a hybrid platform. Turkish Journal of Electrical Engineering and Computer Sciences 2017; 25: 2219-2231. doi: 10.3906/elk-1601-206

[2] Kusum Lata T, Ratna D. Choice of battery energy storage for a hybrid renewable energy system. Turkish Journal of Electrical Engineering and Computer Sciences 2018; 26: 666-676. doi: 10.3906/elk-1707-350

[3] Özçelik MA, Yılmaz AS. Improving the incremental conductance algorithm for two-stage grid-connected photovoltaic systems. Turkish Journal of Electrical Engineering and Computer Sciences 2018; 26: 442-453. doi: 10.3906/elk-1412-119

[4] Bidyadhar S, Raseswari P. A comparative study on maximum power point tracking techniques for photovoltaic power systems. IEEE Transactions on Sustainable Energy 2013; 4: 89-98. doi: 10.1109/TSTE.2012.2202294

[5] Indu Rani B, Saravanailango G, Nagamani C. Impact of partial shading on the output power of PV systems under partial shading conditions. IET Power Electronics 2014; 7: 657-666. doi: 10.1049/iet-pel.2013.0143

[6] Lyden S, Haque ME. A simulated annealing global maximum power point tracking approach for PV modules under partial shading conditions. IEEE Transactions on Power Electronics 2016; 31: 4171-4181. doi: 10.1109/TPEL.2015.2468592

[7] Hiren P, Vivek A. Maximum power point tracking scheme for PV systems operating under partially shaded conditions. IEEE Transactions on Industrial Electronics 2008; 55: 1689-1698. doi: 10.1109/TIE.2008.917118

[8] Mahmoud D. Assessing MPPT techniques on hot-spotted and partially shaded photovoltaic modules: comprehensive review based on experimental data. IEEE Transactions on Electronic Devices 2019; 66: 1132-1144. doi: 10.1109/TED.2019.289400

[9] Jubaer A, Zainal S. A critical evaluation on maximum power point tracking methods for partial shading in PV systems. Renewable and Sustainable Energy Reviews 2015; 47: 933-953. doi: 10.1016/j.rser.2015.03.080

[10] Mohapatra A, Nayak B, Priti D, Mohanty KB. A review on MPPT techniques for PV system under partial shading condition. Renewable and Sustainable Energy Reviews 2017; 80: 854-867. doi: 10.1016/j.rser.2017.05.083

[11] Faiza B, Cherif L. A review of global maximum power point tracking techniques of photovoltaic system under partial shading conditions. Renewable and Sustainable Energy Reviews 2018; 92: 513-553. doi: 10.1016/j.rser.2018.04.094

[12] Guiqiang L, Yi J, Akram MW, Xiao C, Jie Ji J. Application of bio-inspired algorithms in maximum power point tracking for PV systems under partial shading conditions - A review. Renewable and Sustainable Energy Reviews 2018; 81: 840-873. doi: 10.1016/j.rser.2017.08.034

[13] Xingshuo L, Huiqing W, Yihua H, Lin J, Weidong X. Modified beta algorithm for GMPPT and partial shading detection in photovoltaic systems. IEEE Transactions on Power Electronics 2018; 33: 2172-2186. doi: 10.1109/TPEL.2017.2697459

[14] Chakkarapani M, Gururaghav R, Gurupraanesh R, Ganesan S, Nagamani C. A hybrid algorithm for tracking of GMPP based on P&O and PSO with reduced power oscillation in string inverter. IEEE Transactions on Industrial Electronics 2016; 63: 6097-6106. doi: 10.1109/TIE.2016.2590382

[15] Banumalar K, Manikandanbairavan V, Chandrasekaran K, Sishajpulikottil S. Firefly algorithm with multiple workers for the power system unit commitment problem. Turkish Journal of Electrical Engineering and Computer Sciences 2016; 24: 4773–4789. doi: 10.3906/elk-1411-77

[16] Kinattingal S, Vethanayagam V, Peddapati S, Sishaj PS, Srinivasaraonayak P et al. Development of an improved P&O algorithm assisted through a colony of foraging ants for MPPT in PV system. IEEE Transactions on Industrial Informatics 2016; 12: 187-200. doi: 10.1109/TII.2015.2502428

[17] Mohamadamin G, Alireza R, Hossein Iman E. MPPT method for PV systems under partially shaded conditions by approximating I-V curve. IEEE Transactions on Industrial Electronics 2018; 65: 3966-3975. doi: 10.1109/TIE.2017.2764840

[18] Jain S, Agarwal V. Comparison of the performance of maximum power point tracking schemes applied to single-stage grid-connected photovoltaic systems. IET Electric Power Applications 2007; 1: 753-762. doi: 10.1049/iet-epa:20060475

[19] Chao H, Long W, Huan L, Xiong L, Jenq-Haur W. A hybrid global maximum power point tracking method for photovoltaic arrays under partial shading conditions. Optik 2019; 180: 665–674. doi: 10.1016/j.ijleo.2018.11.1

[20] Kueihsiang C. An extension theory-based maximum power tracker using a particle swarm optimization algorithm. Energy Conversion and Management 2014; 86: 435–442. doi: 10.1016/j.enconman.2014.05.018

[21] Hong L, Duo Y, Wenzhe S, Jinhu L, Xinghuo Y. An overall distribution particle swarm optimization MPPT algorithm for photovoltaic system under partial shading. IEEE Transactions on Industrial Electronics 2019; 66: 265-275. doi: 10.1109/TIE.2018.2829668

[22] Hiren P, Vivek A. Maximum power point tracking scheme for PV systems operating under partially shaded conditions. IEEE Transactions on Industrial Electronics 2008; 55: 1689-1698. doi: 10.1109/TIE.2008.917118